Received: 7 May 2021 | Accepted: 1 October 2021
DOI: 10.1002/jcp.30601

RESEARCH ARTICLE

Journal of Cellular Physiology WILEY

Regulation of electrogenic Na^+/HCO_3^- cotransporter 1 (NBCe1) function and its dependence on m-TOR mediated phosphorylation of Ser^{245}

Marina Giannaki[1] | **Christina Ludwig**[2] | **Stephan Heermann**[1] | **Eleni Roussa**[1]

[1]Department of Molecular Embryology, Institute of Anatomy and Cell Biology, Medical Faculty, Albert-Ludwigs-Universität Freiburg, Freiburg, Germany

[2]Bavarian Center for Biomolecular Mass Spectrometry (BayBioMS), Technical University of Munich (TUM), Freising, Germany

Correspondence
Eleni Roussa, Department of Molecular Embryology, Institute for Anatomy and Cell Biology, Medical Faculty, Albert-Ludwigs-Universität Freiburg, Albertstrasse 17, Freiburg D-79104, Germany.
Email: eleni.roussa@anat.uni-freiburg.de

Abstract

Astrocytes are pivotal responders to alterations of extracellular pH, primarily by regulation of their principal acid-base transporter, the membrane-bound electrogenic Na^+/bicarbonate cotransporter 1 (NBCe1). Here, we describe amammalian target of rapamycin (mTOR)-dependent and NBCe1-mediated astroglial response to extracellular acidosis. Using primary mouse cortical astrocytes, we investigated the effect of long-term extracellular metabolic acidosis on regulation of NBCe1 and elucidated the underlying molecular mechanisms by immunoblotting, biotinylation of surface proteins, intracellular H^+ recording using the H^+-sensitive dye 2′,7′-bis-(carboxyethyl)-5-(and-6)-carboxyfluorescein, and phosphoproteomic analysis. The results showed significant increase of NBCe1-mediated recovery of intracellular pH from acidification in WT astrocytes, but not in cortical astrocytes from NBCe1-deficient mice. Acidosis-induced upregulation of NBCe1 activity was prevented following inhibition of mTOR signaling by rapamycin. Yet, during acidosis or following exposure of astrocytes to rapamycin, surface protein abundance of NBCe1 remained -unchanged. Mutational analysis in HeLa cells suggested that NBCe1 activity was dependent on phosphorylation state of Ser^{245}, a residue conserved in all NBCe1 variants. Moreover, phosphorylation state of Ser^{245} is regulated by mTOR and is inversely correlated with NBCe1 transport activity. Our results identify $pSer^{245}$ as a novel regulator of NBCe1 functional expression. We propose that context-dependent and mTOR-mediated multisite phosphorylation of serine residues of NBCe1 is likely to be a potent mechanism contributing to the response of astrocytes to acid/base challenges during pathophysiological conditions.

KEYWORDS
acid-base, acidosis, astrocytes, pH, signaling

1 | INTRODUCTION

Extracellular acidosis is a hallmark of many pathophysiological conditions, including inflammation, ischemia, and solid tumors (Corbet & Feron, 2017; Menyhárt et al., 2017). Extracellular acid load ultimately leads to intracellular acidification, thereby impairing essential pH-sensitive cellular functions and compromising cell survival. A common cellular response to extracellular acid-base disturbances is regulation of membrane acid-base transporters. In the brain, among several H^+/HCO_3^- transport proteins, the electrogenic Na^+/HCO_3^- cotransporter 1 (NBCe1), the product of *Slc4a4* gene, is of particular importance. NBCe1 is highly expressed in astrocytes (Deitmer & Rose, 1996, 2010; Rickmann et al., 2007), capable of sensing bicarbonate, and may operate to transport Na^+ and bicarbonate in the inward or outward mode (Theparambil et al., 2014, 2017). In mouse cortical astrocytes, during short extracellular acid loads of different origin, such as isocapnic acidosis, hypercapnic acidosis and isohydric hypocapnia, NBCe1 operates in the outwardly directed mode (Theparambil et al., 2017). Such an operating mode also applies for recovery of cortical astrocytes from cytosolic alkalosis (Theparambil et al., 2015). In contrast, in pH sensitive astrocytes of the brainstem that are known to express *Slc4a4* at considerably higher levels than cortical astrocytes, CO_2-induced acidification activates inwardly operating NBCe1 that transports Na^+ inside the cell that in turn activates Na^+/Ca^{2+} exchanger (NCX) to operate in a reverse mode leading to Ca^{2+} entry and activation of downstream signaling pathways (Turovski et al., 2016). Notably, intracellular pH responses in different cell types following two sequential metabolic acidosis challenges (i.e., reducing extracellular pH and bicarbonate at constant CO_2) revealed a wide range, suggesting dependence both on the individual cell and cell type (Salameh et al., 2014).

The physiological significance of the action of astrocytic NBCe1 for stabilizing extracellular pH in the brain has been proposed since many years (Deitmer, 1991, 1992) but recently been demonstrated in vitro and in vivo (Theparambil et al., 2020). Astrocytes release bicarbonate to counteract the neuronal activity-associated transient extracellular acid load, thereby protecting the brain milieu from acidification. A crucial player in the molecular machinery underlying this response involves facilitated outward transport of bicarbonate via electrogenic NBCe1. Thus, understanding the molecular mechanisms that regulate NBCe1 activity has high biological relevance. The phosphorylation state of several serine residues has emerged as a potent mechanism regulating NBCe1 function. Phosphorylation of Ser^{232}, Ser^{233}, and Ser^{235} is regulated by IRBIT and determines transporter activity and its sensitivity to Cl^- (Vachel et al., 2018), and phosphorylation of $Ser^{255-257}$ which is regulated by mammalian target of rapamycin (mTOR) regulates NBCe1 functional expression (Khakipoor et al., 2019). Ser^{245} is constitutively phosphorylated as well, but whether this modification has a functional significance on NBCe1 transport activity is not known.

mTOR is an evolutionarily-conserved serine-threonine kinase that regulates cell growth, proliferation, and metabolism (Hsu et al., 2011; Laplante & Sabatini, 2012) and also maintains renal tubular homeostasis (Fantus et al., 2016; Grahammer et al., 2014, 2016, 2017). mTOR operates as at least two distinct, multi-protein complexes: mTOR complex 1 (mTORC1) and mTOR complex 2 (mTORC2). A link between extracellular acidosis and mTOR signaling has been established in the context of tumors and tumor progression. Acidic pH and tumor hypoxia negatively regulate mTORC1 activity (Balgi et al., 2011; Laplante & Sabatini, 2012). Interestingly, whereas mTORC2 is not affected by pH, acidic pH inhibits mTORC1 activity (Balgi et al., 2011; Faes et al., 2016).

In the present study, we show that prolonged extracellular metabolic acidosis upregulates NBCe1 functional expression without changes on protein abundance in astrocytes, a response prevented following inhibition of mTOR signaling. We also identify Ser^{245} as a novel regulator of NBCe1 and demonstrate that mTOR-mediated phosphorylation state of Ser^{245} regulates NBCe1 activity.

2 | MATERIAL AND METHODS

2.1 | Antibodies and reagents/chemicals

Following antibodies were used as primary antibodies: anti-SLC4A4 rabbit polyclonal from Alomone Labs (Cat# ANT-075; RRID: AB_2341019) for western blots; anti-SLC4A4 from Atlas Antibodies (Cat# HPA035628; RRID: AB_2674708) for immunocytochemistry; anti-GAPDH mouse monoclonal from Abcam (Cat# ab8245; RRID: AB_2107448), anti-GFAP mouse monoclonal from Merck Millipore (Cat# MAB360; RRID: AB_11212597) for immunocytochemistry and rabbit polyclonal anti-GFAP from Dako (Cat# Z0334; RRID: AB_10013382) for western blots and anti-Na^+/K^+-ATPase α-1 subunit mouse monoclonal from Millipore (Cat# 05-369; RRID: AB_310154). For immunofluorescence donkey anti-rabbit AlexaFluor594, from Dianova (Cat# 711-585-152; RRID: AB_2340621) or donkey anti-mouse AlexaFluor488 (Cat# 715-545-151; RRID: AB_2341099) were used as secondary antibodies. For western blots, goat-anti-mouse or anti-rabbit IgG coupled to horseradish peroxidase from Jackson ImmunoResearch Labs (Cat# 715-475-151; RRID:AB_2340840) or from Thermo Fisher Scientific (Cat# A10042; RRID: AB_2534017) were used as secondary antibodies. Ethylisopropyl amiloride (EIPA), and rapamycin were purchased from Tocris Bioscience (Cat# 3378, and Cat#1292, respectively), 3-benzyl-5-((2-nitrophenoxy)methyl)-dihydrofuran-2(3H)-one (3BDO) and S0859 from Sigma-Aldrich (Cat# SML1687 and Cat# SML0638, respectively) and BCECF-AM from Thermo Fisher Scientific (Cat# B8806).

2.1.1 | Animals

All protocols were carried out in accordance with German ethical guidelines for laboratory animals and approved by the Institutional Animal Care and Use Committee of the University of Freiburg (authorizations: X14/16H and X19/09C). Adult C57BL/6N mice (strain code 027) of either sex were maintained on a 12 h dark/light cycle with food and water ad libitum. Mice were sacrificed by cervical dislocation, and all efforts were made to minimize suffering. *Slc4a4* deficient mice have been described earlier (Gawenis et al., 2007).

2.2 | Cell culture

2.2.1 | Mouse primary hippocampal and cortical astrocyte cultures

For primary culture of mixed glia, mouse pups aged P2/P3 were used, as previously described (Khakipoor et al., 2017, 2019). Cortices and hippocampi were dissected and immediately collected in cold HBSS on ice. After application of trypsin and incubation at 37°C for 30 min, probes were centrifuged for 5 min at 1300 rpm and supernatant was removed. Pellets were resuspended in plating medium (DMEM) and vigorously pipetted (20–30 times) to obtain single cell suspensions. Single cells were then plated on poly-D-lysine coated 25 cm^2 flasks or coverslips in petri dishes. Culture medium was changed every second day and experiments were carried out after 15–21 days in vitro. Culture medium was replaced by medium adjusted to pH 7.4, or 6.8 with 26 mM, or 6.1 mM $NaHCO_3$, respectively, in the presence or absence of 1 µM rapamycin for different time periods at 37°C in a 5% CO_2 incubator. To preserve osmolarity, 19.9 mM NaCl was added to the culture medium of pH 6.8 and osmolarity was further measured using an osmometer. Culture media were allowed to equilibrate for approximately 48 h at 37°C in a 95% O_2/5% CO_2 incubator prior the experiments. Subsequently, cultures were processed for immunoblotting, surface biotinylation of proteins or intracellular H^+ recordings.

2.3 | 3-(4,5-Dimethylthiazol-2-yl)-2,5-diphenyltetrazolium bromide (MTT) assay

Control cortical astrocytes and those exposed to extracellular acidosis for different time periods were incubated with 1 mg/ml MTT (Cat# M6494; Thermo Fisher Scientific), for 4 h at 37°C in a 95% O_2/5% CO_2 incubator, according to the manufacturer's protocol. Color intensity of the produced formazan was measured using a Vector microplate reader (PerkinElmer) (Liu et al., 1997). All treatments were performed in triplicate.

2.4 | Immunoblotting

Primary cortical or hippocampal astrocytes were harvested and homogenized, and protein concentration was determined by Thermo Fisher Scientific NanoDrop 2000 spectrophotometer (at absorbance 280 nm). Electrophoresis and blotting procedures were performed as described (Khakipoor et al., 2017). Primary antibodies were diluted as follows: NBCe1 1:2000–1:5000, GAPDH 1:10,000–1:20,000, GFAP 1:20,000, and Na^+/K^+-ATPase 1:5000. Blots were developed in enhanced chemiluminescence reagents and signals were visualized on X ray films. Subsequently, films were scanned and the signal ratio NBCe1:GAPDH, NBCe1:Na^+/K^+-ATPase, and GFAP:GAPDH was quantified densitometrically. Differences in signal ratio were tested for significance using either two-tailed unpaired Student's *t* test or one-way analysis of variance (ANOVA) and Bonferroni posthoc test. Results with levels of $^*p < 0.05$ were considered significant.

2.5 | Cell surface biotinylation

Primary cortical astrocytes were subjected to control or extracellular metabolic acidosis for 30 min, 3 or 6 h in the presence or absence of 1 µM rapamycin and then kept on ice. Isolation of cell surface proteins was performed using the Pierce® cell surface protein isolation kit following the manufacturer's instructions. Probes were then processed for immunoblotting with antibodies against NBCe1, Na^+/K^+-ATPase, and GAPDH, as described above or for quantitative phosphoproteomic analysis.

2.5.1 | Intracellular H^+ imaging in cortical astrocytes

To measure intracellular H^+ concentration ($[H^+]_i$) changes in cultured cortical astrocytes in the presence or absence of rapamycin, we used a Visitron imaging system (http://www.visitron.de/) and the acetoxymethyl ester of a proton-sensitive dye, 2′,7′-bis-(carboxyethyl)-5-(and-6)-carboxyfluorescein (BCECF-AM), as described previously (Giannaki et al., 2021; Khakipoor et al., 2017, 2019). Cells were incubated with 3 µM BCECF-AM in bicarbonate-buffered saline solution for 15 min at room temperature. Cells were then mounted on a chamber of the Nikon ECLIPSE TE200 microscope and perfused continuously at room temperature with CO_2/HCO_3^--buffered saline solutions (in mM): NaCl 116, KCl 3, NaH_2PO_4 0.5, α-D-glucose 2, $NaHCO_3$ 26, $MgCl_2$ 1, and $CaCl_2$ 2, pH 7.4 or NaCl 135.9, KCl 3, NaH_2PO_4 0.5, α-D-glucose 2, $NaHCO_3$ 6.1, $MgCl_2$ 1, and $CaCl_2$ 2, pH 6.8. BCECF was excited consecutively at 488 nm (proton-sensitive wavelength) and 440 nm (close to isosbestic point), and the changes in fluorescence emission were monitored at >505 nm (using ET540/40 m filter). Images were obtained every 10 s with a ×20 objective. The fluorescence emission intensity of 488 nm excitation changes inversely with a change in $[H^+]_i$, whereas the fluorescence emission intensity of 440 nm excitation is largely pH insensitive. The changes in $[H^+]_i$ were monitored using the ratio $F(440)/F(488)$. The ratio was converted into pH and absolute intracellular proton concentrations ($[H^+]_i$) by using the nigericin-based (4 µM) calibration technique (Khakipoor et al., 2017; Theparambil et al., 2014). Cells were perfused with calibration solution containing (in mM): KCl 145, NaH_2PO_4 0.4, Na_2HPO_4 1.6, Glucose 5, $MgCl_2$ $6H_2O$ 1, Ca-DiGluconat H_2O 1.3, adjusted at pH 6.5, 7.0, 7.5, and 8.0.

2.6 | Constructs and transfection of HeLa cells

The wild type (WT) construct from NBCe1 (*Slc4a4*) sequence (NM_018760) was designed, established, and described previously (Khakipoor et al., 2019). The NBCe1 sequence was introduced to a backbone of the pEGFP-C1 vector (Clontech) according to Yang et al. (2009). Another WT construct was designed and established in which the fluorescent protein coding sequence of green fluorescent protein (GFP) was replaced by mCherry (Figure S1a). Mutant constructs from NBCe1 (*Slc4a4*) sequence (NM_018760) were designed with Geneious version 10.0 (created by Bio matters, www.geneious.com). The coding sequence for aa 245, of the WT NBCe1 was altered from AGC, coding for a serine, to GCC in NBCe1-B-S245A, coding for an alanine, mimicking the dephosphorylated status, and to GAC, in NBCe1-B-S245D, coding for an aspartate, mimicking the phosphorylated status. The constructs were generated by site directed mutagenesis by GeneCust (Luxembourg), using the following forward (F) and reverse (R) primers:

Primers spanning the mutation site, used for both constructs, NBCe1-B-S245A and NBCe1-B-S245D were:

Primer 1 F: CTCAGATCTCGAGCTCAAGCTTCGAATTCAATG GAGGATGAAGCTGTCCTGG

Primer 1 R: GAGAATGAAGGACATGAGTGTGATATCAGGCACG AAGTCACAGTTG

Primers harboring the mutation site for construct NBCe1-B-S245A were:

Primer A, F: GTTTAGCAACCCTGATAATGGCGCCCCAGCCATG ACCCACAGGAATC

Primer A, R: CCTGTGGGTCATGGCTGGGGCGCCATTAT CAGGGTTGCTAAACATCC

Primers harboring the mutation site for construct NBCe1-B-S245D were:

Primer D, F: GCAACCCTGATAATGGCGACCCAGCCATGACCC ACAGGAATCTGACA

Primer D, R: GATTCCTGTGGGTCATGGCTGGGTCGCCATTAT CAGGGTTGCTAAACA

The results were verified by sequencing.

HeLa cells grown on coverslips were transfected with 500 ng/ml of WT-NBCe1-B (either eGFP or mCherry), NBCe1-B-S245A or NBCe1-B-S245D constructs using Lipofectamine P3000 (Thermo Fisher Scientific), following the manufacturer's instructions. Culture medium was replaced by medium adjusted to pH 7.4 (containing 26 mM $NaHCO_3$) after 24 h of transfection. Intracellular H^+ imaging was performed 48 h after transfection. To identify the transfected cells, images were taken using a ×20 air objective before loading the cells with BCECF dye. For quantification of mean eGFP or mCherry intensity in the experimental conditions, regions of interest were defined and intensity was compared using Visitron imaging software. Background subtraction was applied to all the images.

2.7 | Immunocytochemistry

Primary cortical astrocytes or HeLa cells transfected with WT-NBCe1-B, NBCe1-B-S245A or NBCe1-B-S245D constructs were fixed with 4% PFA for 30 min at room temperature. Cells were washed with PBS and treated with 1% SDS for 5 min, blocked with 1% BSA and incubated with primary antibody α-NBCe1 (1:200 diluted in BSA) or α-GFAP diluted 1:1000 in PBS overnight at 4°C. Cells were washed with PBS, and incubated with goat anti-rabbit IgG coupled to Alexa 594 (1:400) or goat anti-mouse IgG coupled to Alexa 488 (1:400) for 1 h. Coverslips were washed with PBS and mounted with Fluoromount-G, containing 4',6'-diamidino-2-phenylindole dihydrochloride (#0100-20; SouthernBiotech) for nuclear staining. Images were acquired with a Leica TCS SP8 confocal microscope using a HC PL APO CS2 63x/1.40 oil objective lens.

2.8 | Intracellular pH measurements in HeLa cells

Intracellular pH measurements in HeLa cells were performed essentially as previously described (Khakipoor et al., 2019). Cells were perfused at room temperature with CO_2/HCO_3^--buffered solution (in mM): NaCl 115, KCl 5, α-D-glucose 10, $NaHCO_3$ 25, $MgCl_2$ 1, and $CaCl_2$ 1, pH 7.4. For intracellular acidification, cells were perfused with 20 mM NH_4Cl in a Na^+-free bath solution. NBCe1 cotransporter activity was initiated by perfusing HeLa cells with HCO_3^--buffered solution containing 140 mM Na^+. In Na^+-free HCO_3^--buffered solutions, NaCl, and/or $NaHCO_3$ were replaced with equimolar concentrations of *N*-methyl-D-glucamine-Cl, and choline bicarbonate, respectively. All solutions were adjusted to pH 7.4. NBCe1 cotransporter activity was calculated from the slope of change in pH_i/min (pH_i recovery rate after acidification). Further, NBCe1 cotransporter activity was measured by incubating cells with 10 µM EIPA to inhibit all Na^+-H^+ exchangers according to previous reports (Hong et al., 2013; Yang et al., 2011), in Na^+-free HCO_3^--buffered solution, and in the presence or absence of either 1 µM rapamycin or 60 µM 3BDO, an inhibitor (Kuo et al., 1992) and activator (Ge et al., 2014) of mTOR signaling, respectively. Only cells with the same GFP or mCherry intensity were considered for quantification.

2.9 | Phosphoproteomic analysis

After surface-proteome enrichment all samples were dissolved in 1× NuPAGE™ LDS sample buffer (Thermo Fisher Scientific). In-gel trypsin digestion was performed according to standard procedures (Shevchenko et al., 2006). Briefly, the samples were run on a NuPAGE™ 4%–12% Bis-Tris protein gel (Thermo Fisher Scientific) for 5 min. Subsequently, the still not size-separated single protein band per sample was cut, reduced (50 mM dithiothreitol), alkylated (55 mm chloroacetamide) and digested overnight with trypsin (Trypsin Gold; Promega). LC-MS/MS measurements were performed on an Ultimate 3000 RSLCnano system coupled to a Q-Exactive HF-X mass spectrometer (Thermo Fisher Scientific). The Q-Exactive HF-X mass spectrometer was operated in data dependent acquisition and positive ionization mode. Peptide identification and quantification was performed using the software MaxQuant (version 1.6.17.0) with its built-in search engine Andromeda (Cox et al., 2011; Tyanova et al., 2016). MS2 spectra were searched against the mus musculus reference protein database from UniProt (UP000000589, 17038 reviewed protein entries, download 17.7.2020), supplemented with common contaminants (built-in option in MaxQuant). Trypsin/P was specified as proteolytic enzyme. Carbamidomethylated cysteine was set as fixed modification. Phosphorylation on serine, threonine and tyrosine was specified as variable modification, as well as oxidation of methionine and acetylation at the protein N-terminus. Results were adjusted to 1% false discovery rate on peptide spectrum match level and protein level employing a target-decoy approach using reversed protein sequences. A targeted quantitative analysis of all identified NBCe1 peptides (phosphopeptides as well as naked peptides) was performed using the software Skyline (MacLean et al., 2010). Extracted precursor ion chromatograms were integrated and the resulting NBCe1 phosphopeptide intensities were normalized to the total NBCe1 protein intensity (summed up intensities of all naked peptides) in each sample respectively. The corresponding Skyline document, as well as all proteomic raw data and MaxQuant search results have been deposited to Panorama Public (Sharma et al., 2018) and are freely accessible under https://panoramaweb.org/NBCe1_phospho.

3 | RESULTS

3.1 | Extracellular metabolic acidosis does not affect NBCe1 protein abundance in mouse hippocampal and cortical astrocytes

Previous studies have shown that short-term, acute extracellular acid load and long-term extracellular alkalosis in astrocytes evoke intracellular pH (pH_i) responses, mainly mediated by the action of NBCe1 (Khakipoor et al., 2019; Theparambil et al., 2017). We have investigated whether a prolonged extracellular acid load caused by a decrease in bicarbonate concentration ($[HCO_3^-]_o$) and pH at constant CO_2 (i.e., mimicking metabolic acidosis) regulates protein expression of NBCe1. Therefore, primary mouse hippocampal and cortical astrocytes were exposed to extracellular acidosis (Ac, pH_o 6.8; 6.1 mM HCO_3^-) from 30 min to 6 h and subsequently NBCe1 protein abundance was determined by immunoblot analysis. Using an antibody raised against NBCe1, immunoreactive bands at ~110 kDa and ~130 kDa were detected in controls (Figure 1a,b lane 1), as previously described (Khakipoor et al., 2019). Quantification showed at all experimental conditions no significant changes in total NBCe1 protein abundance, compared to control astrocytes exposed to extracellular pH 7.4. For cortical astrocytes (Figure 1a): 0.96 ± 0.08-, 1.00 ± 0.11-, 1.09 ± 0.09-, 0.92 ± 0.08-, 0.98 ± 0.05-, 1.01 ± 0.08-, and 0.98 ± 0.11-fold for controls and exposure to acidosis for 30 min, 1, 2, 3, 4, and 6 h, respectively, not significant using two-tailed unpaired Student's *t* test, n = 3–6). For hippocampal astrocytes (Figure 1b): 1.00 ± 0.18-, 1.30 ± 0.07-, 1.14 ± 0.14-, 1.08 ± 0.11-, 1.15 ± 0.08-, 1.03 ± 0.17-, and 1.23 ± 0.05-fold, for controls and exposure to acidosis for 30 min, 1, 2, 3, 4, and 6 h, respectively, not significant using two-tailed unpaired Student's *t* test, n = 3)

3.2 | Extracellular metabolic acidosis does not alter trafficking of NBCe1 in the cell membrane, cell survival, or activation state of cortical astrocytes

Extracellular acidosis may induce recruitment of acid-base transporters to the plasma membrane as an adaptive mechanism to pathological challenge (Oehlke et al., 2011, 2012, 2013). In cortical astrocytes, however, surface NBCe1 protein expression was not significantly altered following exposure to extracellular metabolic acidosis for either 30 min, 3 or 6 h (Figure 2a; 1.00 ± 0.08-, 1.01 ± 0.08-, 1.05 ± 0.09-, and 1.09 ± 0.09-fold for control, 30 min, 3 and 6 h exposure to acid load, respectively, not significant, using, two-tailed unpaired Student's *t* test, n = 3–5). Lack of GAPDH protein abundance in the samples demonstrated enrichment of surface proteins. Moreover, viability of control and acidotic astrocytes, as tested by MTT assay, was comparable. As shown in Figure 2b, astrocytes revealed a viability of 96.64 ± 3.97%, 108.7 ± 9.06%, and 100.3 ± 3.56%, following exposure to extracellular acidosis, for 30 min, 3 and 6 h, respectively (n = 3–4), thus showed no significant differences compared to the untreated controls (using one-way ANOVA and Bonferroni posthoc test).

Subsequently, to determine whether extracellular metabolic acidosis may induce regulation of astrocytic activation markers (Pekny & Nilsson, 2005), GFAP protein abundance was determined by immunoblotting (Figure 2c). An immunoreactive band at ~50 kDa was detected in controls and showed no significant changes in all experimental groups investigated (1.00 ± 0.11-, 1.02 ± 0.08-, 1.05 ± 0.10-, 1.08 ± 0.18-, 1.09 ± 0.20-, 0.97 ± 0.06-, and 1.19 ± 0.33-fold for controls and exposure to acidosis for 30 min, 1, 2, 3, 4, and 6 h, respectively, not significant using two-tailed unpaired Student's *t* test, n = 4–6).

These results were further confirmed by immunofluorescence for GFAP (Figure 2d). Consistent with the immunoblot data, no differences on GFAP labelling intensity (green) were observed in all experimental conditions investigated. However, due to the high variation of GFAP protein abundance after 6 h exposure to acidosis (Figure 2c) and to ensure that the subsequent experiments on NBCe1 transport activity are not performed in astrocytes that might have acquired molecular properties of astrocytic activation, we have selected the 3 h exposure to acidosis for the next experiments.

3.3 | Extracellular acidosis regulates NBCe1 transport activity in cortical astrocytes

Previous work has shown that long-term metabolic alkalosis downregulates transport activity of NBCe1 without altering total or surface protein expression levels (Khakipoor et al., 2019). With this background in mind, we asked whether metabolic acidosis (i.e., decreased extracellular $[HCO_3^-]$ and pH at constant CO_2) for 3 h regulates NBCe1 transport activity as well. Intracellular $[H^+]$ recordings have been performed and $[H^+]_i$ was monitored in cultured WT (WT, *Slc4a4*$^{+/+}$) (Figure 3a,b) and *Slc4a4* deficient (Figure 3c,d; NBCe1 KO) cortical control (exposed to pH 7.4) astrocytes and in acidosis-treated astrocytes loaded with the H^+-selective dye BCECF. NBCe1 activity was challenged by increasing the pH value and $[HCO_3^-]$ of the external solution from 6.8 and 6.1 mM to 7.4 and 26.0 mM, respectively. This activates NBCe1 to transport Na^+-HCO_3^- into the cells, which results in a decrease of $[H^+]_i$. This decrease in $[H^+]_i$, was determined in control (Figure 3a) and in acidosis-treated astrocytes (Figure 3b). Using this experimental design, the rate of alkalinisation in pH 6.8 (Figure 3a,b,f) and the rate of acidification upon returning from pH 7.4 to pH 6.8 (Figure 3a,b,e) was measured. Whereas the rate of acidification was comparable between the groups (Figure 3e;

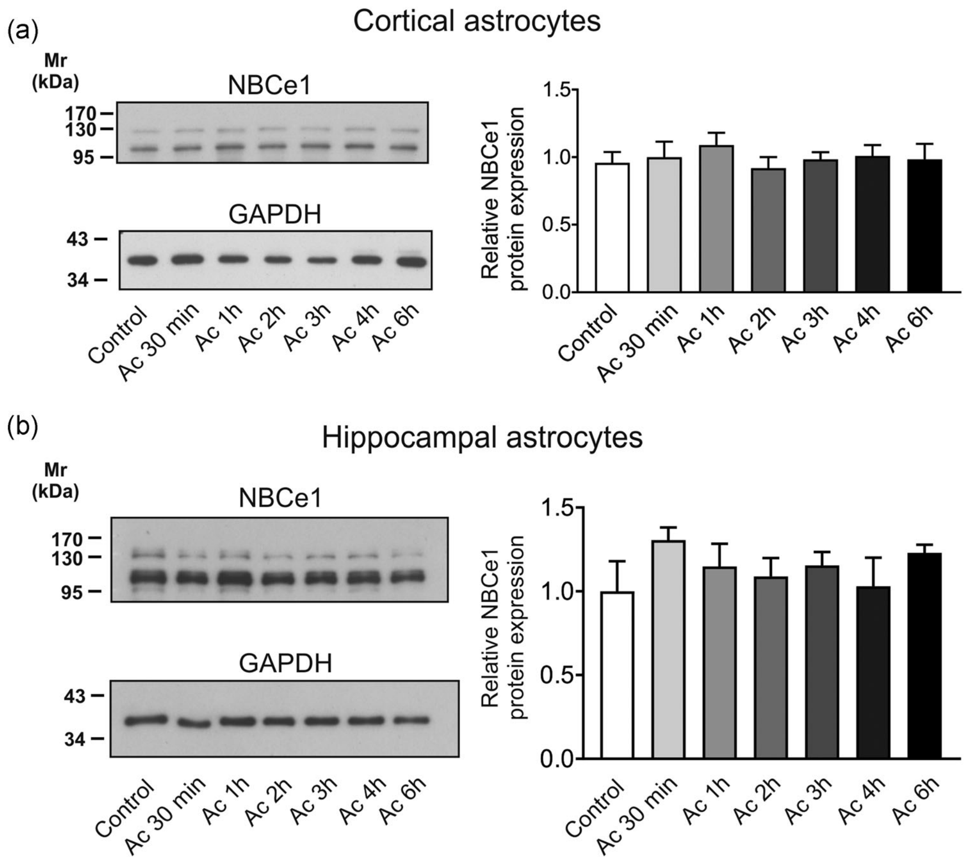

FIGURE 1 NBCe1 protein abundance is not regulated following extracellular metabolic acidosis in mouse primary cortical or hippocampal astrocytes. Protein abundance of NBCe1 by immunoblotting in primary cortical (a) and hippocampal (b) astrocytes following extracellular metabolic acidosis (Ac, pH_o 6.8) from 30 min to 6 h. Not significant after densitometric analysis of the signal ratio NBCe1 (~110 and ~130 kDa bands): GAPDH and two-tailed unpaired Student's *t* test. Thirty microgram protein was loaded per lane. Data are presented as mean ± SEM, normalized to the mean of control. The blots are representative of 3–6 different experiments. NBCe1, Na^+/bicarbonate cotransporter 1

153.5 ± 9.66 nM/min and 170.9 ± 9.01 nM/min for acidotic and control astrocytes, respectively), a significant increase in the rate of alkalinization (Figure 3f) was induced after extracellular acidosis for 3 h (−527.0 ± 23.08 nM/min) compared to control (−428.5 ± 25.00; $^{**}p < 0.01$, using the two-tailed unpaired Student's *t* test) (Figure 3e,f).

In NBCe1-KO control (Figure 3c), as well as in acidotic (Figure 3d) astrocytes, the rate of alkalinisation (Figure 3f; −10.91 ± 2.89 nM/min and −17.82 ± 2.41 nM/min, respectively) and the rate of acidification (Figure 3e; 13.62 ± 1.39 nM/min and 15.08 ± 1.81 nM/min, respectively) were greatly reduced as compared to WT cells. These results are in agreement with previous studies where NBCe1-KO cells when changing the perfusion solutions with lower [HCO_3^-] and pH values, reversibly acidified much less and more slowly, compared to WT astrocytes (Theparambil et al., 2017).

3.4 | NBCe1 transport activity depends on the phosphorylation status of Ser^{245}

We have previously shown that mTOR-mediated phosphorylation of $Ser^{255\text{-}257}$ correlates with increased NBCe1 functional expression (Khakipoor et al., 2019). Moreover, acidosis impairs activation of mTOR signaling in several cellular paradigms (Balgi et al., 2011; Laplante & Sabatini, 2012). With this background in mind and based on the results shown in Figure 3, where NBCe1 activity is increased following exposure to acidosis, we have hypothesized that mTOR-regulated phosphorylation of other serine residues of NBCe1 might be inversely correlated with NBCe1 transport activity. NBCe1-B is phosphorylated at several serine residues, among them Ser^{245}. Moreover, we have previously shown that phosphorylation of Ser^{245} revealed the highest occupancy, compared to other serine residues, such as the $Ser^{255\text{-}257}$ and Ser^{232} Ser^{233} Ser^{235} (Khakipoor et al., 2019).

To investigate whether phosphorylation of Ser^{245} has an impact on NBCe1 transport activity, HeLa cells were transfected either with WT-NBCe1-B, or NBCe1-B-S245A (mimicking the dephosphorylated state) or NBCe1-B-S245D (mimicking the phosphorylated state) (Figure 4a) and NBCe1 transport activity was determined. Considering the pH sensitivity of GFP and the similar fluorescence excitation and emission wavelengths between GFP and BCECF we have first excluded that emission of GFP fluorescence is interfering with measurement of WT-NBCe1-B activity using the BCECF dye. HeLa cells were transfected either with WT-NBCe1-B-GFP or with

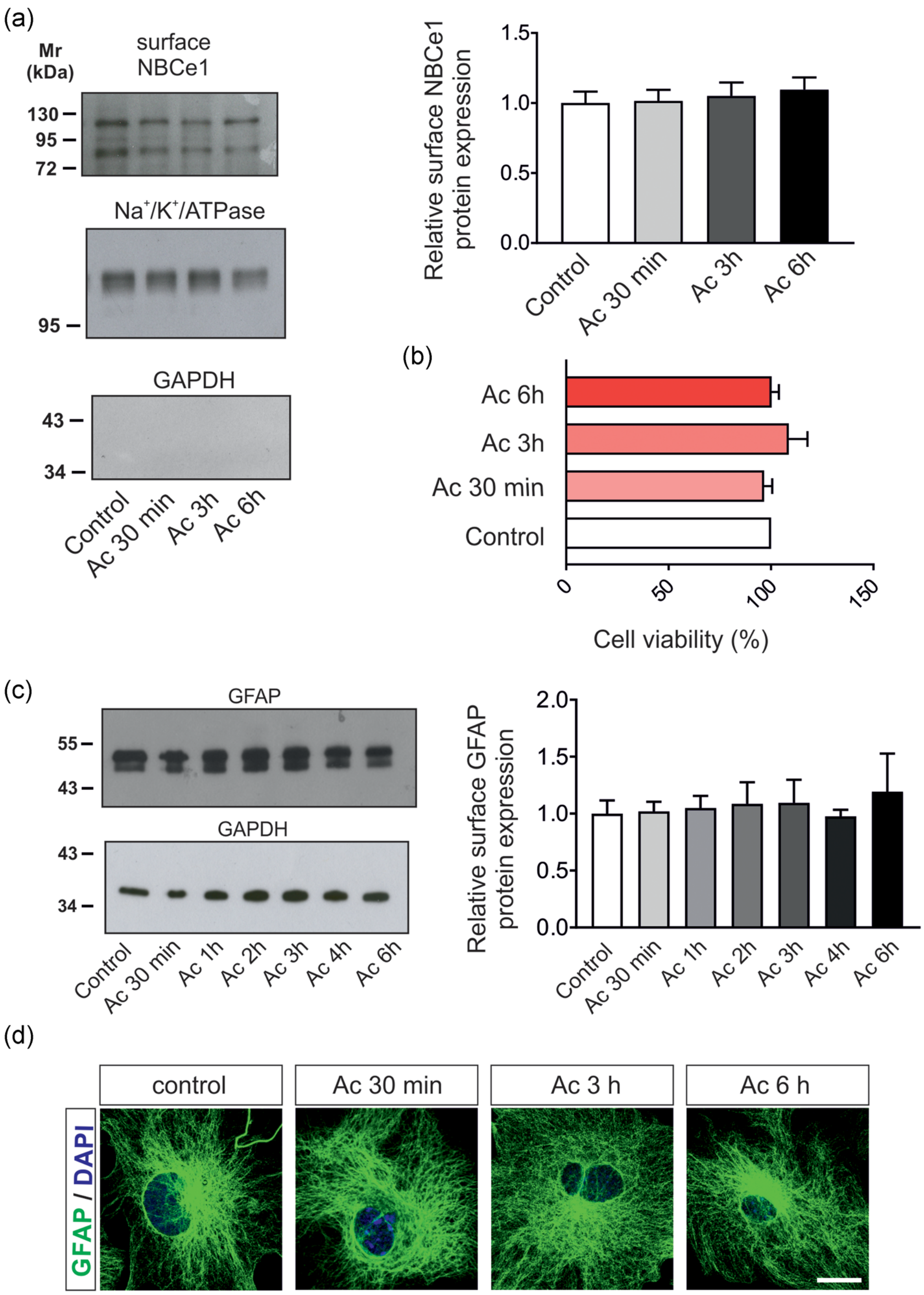

FIGURE 2 Surface NBCe1 abundance, cell viability and expression of astrocytic activation markers following exposure of cortical astrocytes to extracellular acidosis for different time periods. (a) Immunoblot analysis of enriched cell surface proteins for NBCe1 in control primary cortical astrocytes and those exposed to metabolic acidosis for 30 min, 3 or 6 h. Not significant after densitometric analysis of the signal ratio NBCe1: Na^+/K^+-ATPase and two-tailed unpaired Student's *t* test, *n* = 3–5. Eighty microgram protein was loaded per lane. Data are presented as mean ± SEM, normalized to the mean of control. (b) Viability of mouse cortical astrocytes was quantified with the MTT assay. Data are given as relative numbers (%) following extracellular acidosis, compared to the untreated controls (not significant, using one-way ANOVA and Bonferroni post hoc test, *n* = 3–4). (c) Immunoblot analysis for GFAP in control primary cortical astrocytes and those exposed to metabolic acidosis (Ac, pH_o 6.8) from 30 min to 6 h. Not significant after densitometric analysis of the signal ratio GFAP: GAPDH and unpaired Student's *t* test, *n* = 4–6. Fifteen microgram protein was loaded per lane). Data are presented as mean ± SEM, normalized to the mean of control. (d) Immunofluorescence for GFAP (green) in mouse cortical astrocytes following extracellular acidosis for different time points. Nuclei are stained with DAPI. Scale bar = 20 µm. ANOVA, analysis of variance; DAPI, 4',6'-diamidino-2-phenylindole dihydrochloride; GFAP, glial fibrillary acidic protein; MTT, 3-(4,5-dimethylthiazol-2-yl)-2,5-diphenyl-tetrazolium bromide; NBCe1, Na^+/bicarbonate cotransporter 1

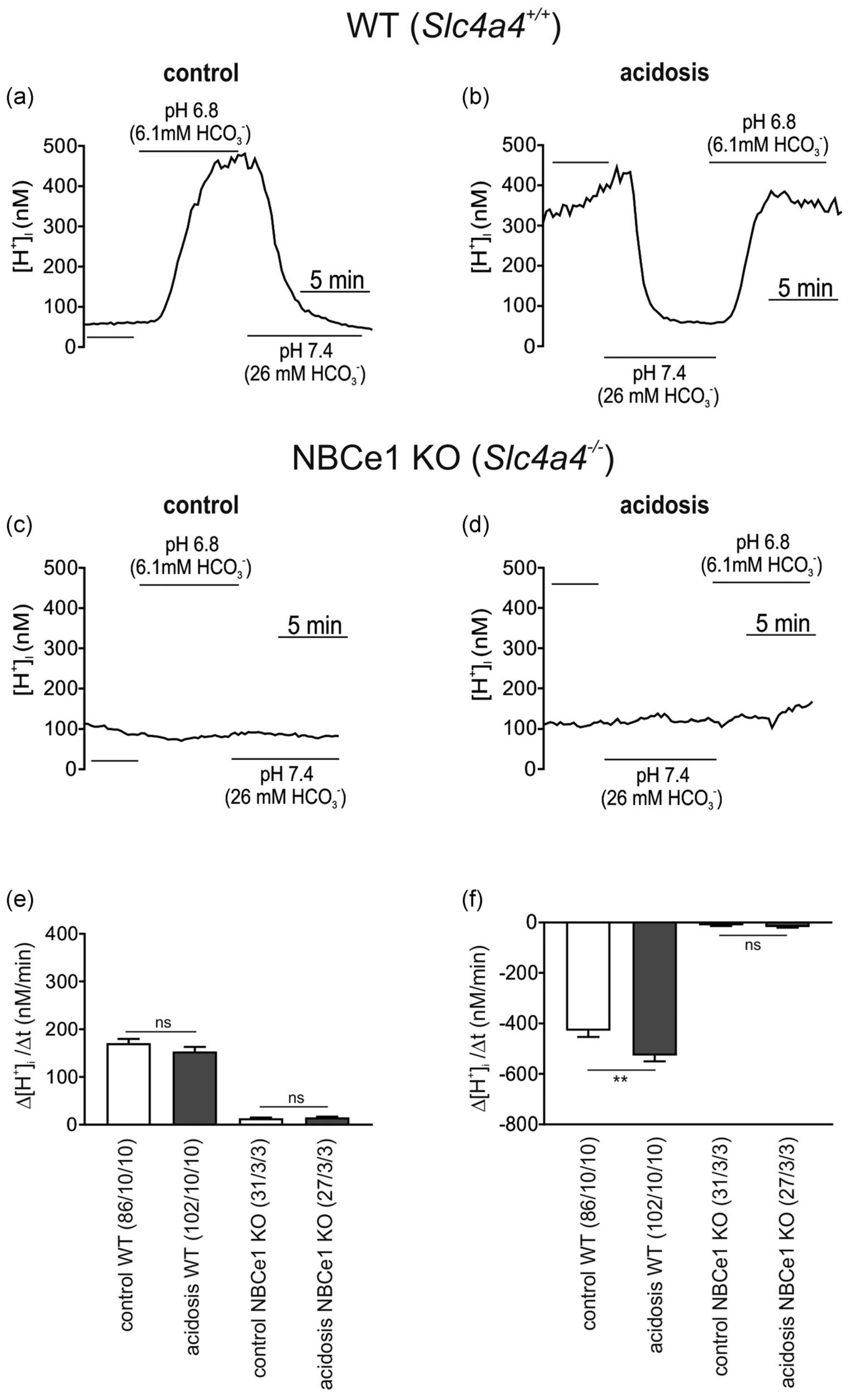

FIGURE 3 Evaluation of NBCe1 transport activity. (a–d) Original recordings of intracellular $[H^+]$ ($[H^+]_i$) in cultured control cortical astrocytes and in astrocytes that have been exposed to extracellular metabolic acidosis for 3 h from WT (a, b) and *Slc4a4* deficient mice (NBCe1-KO; c, d). Original recordings of ($[H^+]_i$ during decrease of external pH and $[HCO_3^-]$ from 7.4 and 26.0 mM to 6.8 and 6.1 mM, respectively, and during increase of external pH and $[HCO_3^-]$ from 6.8 and 6.1 mM to 7.4 and 26.0 mM. (e, f) Bar plots showing the rate of acidification (e) and alkalinisation (f) as measured upon changing external pH and $[HCO_3^-]$ to 6.8 and 6.1 mM, respectively, and back to pH 7.4 and 26.0 mM $[HCO_3^-]$. $^{**}p < 0.01$ for significant increase compared to the controls, using the two-tailed unpaired Student's *t* test. The number of cells/cultures/animals used in the experiments is indicated in brackets. NBCe1, Na^+/bicarbonate cotransporter 1; WT, wild type

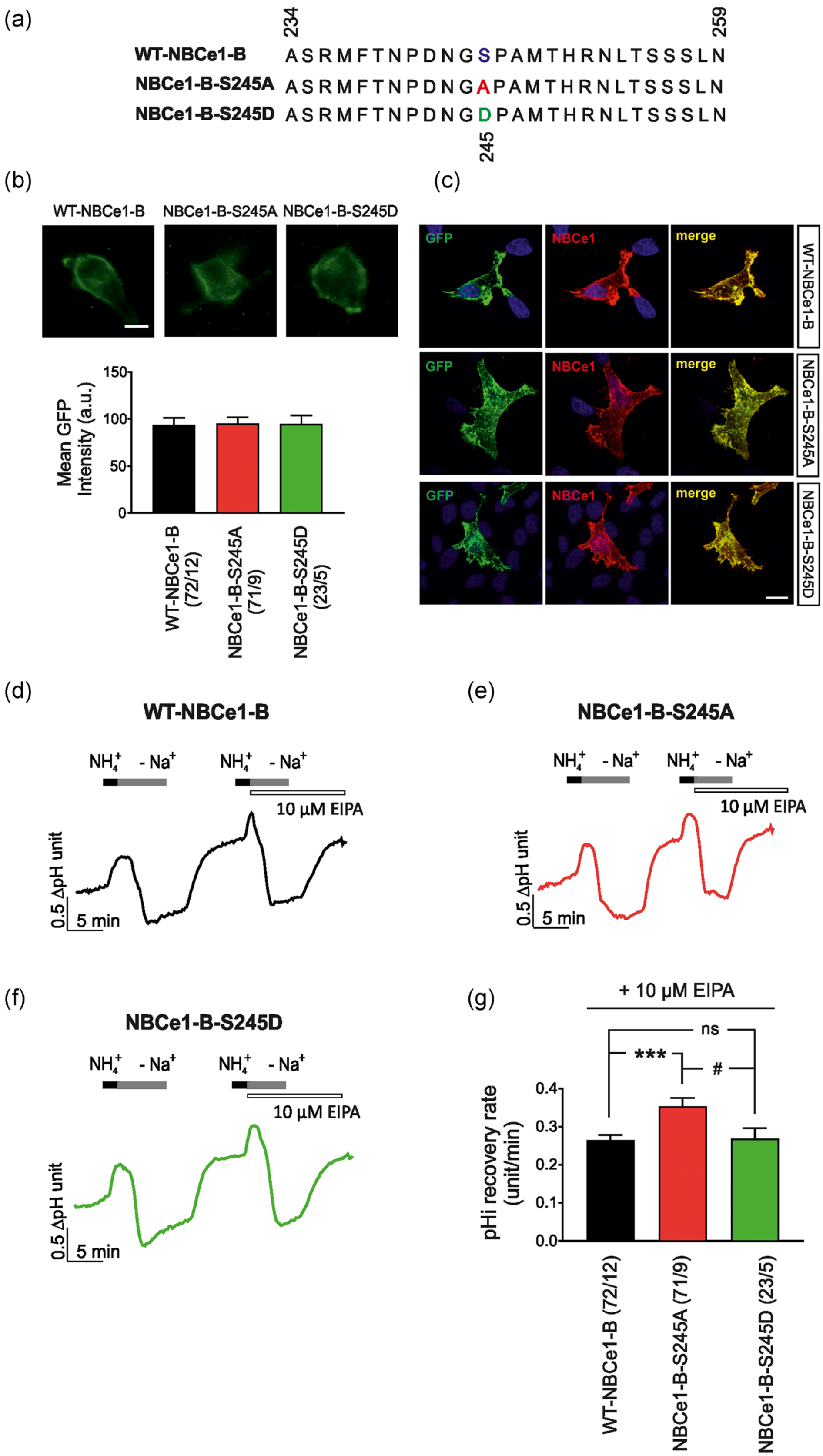

FIGURE 4 (See caption on next page)

WT-NBCe1-B-mCherry (Figure S1a) and the amount of NBCe1 has been determined in GFP- and mCherry-transfected cells by quantification of mean fluorescence intensity (Figure S1b). No significant differences were detected between the groups (128.00 ± 11.11 and 134.50 ± 10.51, for WT-NBCe1-B-mCherry and WT-NBCe1-B-GFP, respectively, using two-tailed unpaired Student's *t*-test). Subsequently, rate of intracellular pH (pH_i) recovery from intracellular acidosis (Figure S1c) was determined. Intracellular acidosis was evoked by a NH_4^+ pulse in Na^+-free solution and pH_i recovery was induced at normal pH 7.4 when Na^+ was added to the perfusion solution and in the presence or absence of 10 µM EIPA. Indeed, pH_i recovery rate was similar between the groups (in the absence of EIPA: 0.38 ± 0.02, and 0.42 ± 0.03, for WT-NBCe1-B-GFP and WT-NBCe1-B-mCherry, respectively, in the presence of EIPA: 0.27 ± 0.01 and 0.27 ± 0.01, for WT-NBCe1-B-GFP and WT-NBCe1-B-mCherry, respectively, not significant, using two-tailed unpaired Student's *t* test). Moreover, as shown in Figure S1d, application of 30 µM of S0859, an inhibitor of NBCe1 (Ch'en et al., 2008), prevented pH_i recovery from intracellular acidification. Based on these results, we have used the GFP-NBCe1 WT and mutant constructs for the subsequent experiments. Again, we have assured that the amount of NBCe1 is comparable between WT- and mutant-transfected cells by quantification of mean GFP intensity (Figure 4b; 93.96 ± 7.50, 95.02 ± 6.76, and 94.75 ± 9.18, for WT, NBCe1-B-S245A and NBCe1-B-S245D, respectively, not significant using two-tailed unpaired Student's *t* test). In addition, immunofluorescence analysis of NBCe1 showed comparable labeling intensity and complete overlap with GFP in WT- and mutant-transfected HeLa cells (Figure 4c). Intracellular pH (pH_i) recordings in WT- and mutant-transfected cells (Figure 4d–f) showed that in the presence of 10 µM EIPA, pH_i recovery was consistently observed in cells transfected with WT-NBCe1-B, with a pH_i recovery rate of 0.26 ± 0.01 pH units/min (Figure 4d,g), whereas in the cells transfected with the NBCe1-B-S245A (Figure 4e,g), pH_i recovery rate after addition of Na^+ was significantly increased (0.35 ± 0.02 pH units/min $^{***}p < 0.001$). In contrast, in cells transfected with NBCe1-B-S245D (Figure 4f,g), pH_i recovery rate (0.27 ± 0.02 pH units/min) revealed no differences compared to the WT, but was significantly decreased compared to NBCe1-B-S245A, $^{\#}p < 0.05$ for significant decrease, using one way ANOVA and Bonferroni posthoc test).

3.5 | mTOR pathway regulates phosphorylation state of Ser^{245}

As a next step, we asked whether phosphorylation of Ser^{245} is mediated by mTOR. Therefore, the impact of either inhibition or activation of mTOR on NBCe1-B-S245A transport activity has been determined. HeLa cells were transfected with WT-NBCe1-B or with NBCe1-B-S245A in the presence or absence of either rapamycin or 3BDO, an inhibitor and activator of mTOR, respectively. As shown in Figure 5a, the amount of transfected WT-NBCe1-B and NBCe1-B-S245A construct within each group, that is, in the presence or absence of rapamycin, and in the presence or absence of 3BDO was comparable in the cells examined, as determined by assessment of GFP intensity. In the presence of rapamycin, no significant differences in GFP intensity could be observed between HeLa cells transfected with WT-NBCe1-B (1.08 ± 0.07-fold) and NBCe1-B-S245A (0.96 ± 0.05-fold; not significant, using the two-tailed unpaired Student's *t* test). Similarly, in the presence of 3BDO, no significant differences in GFP intensity could be observed between HeLa cells transfected with WT-NBCe1-B (1.04 ± 0.08-fold) and NBCe1-B-S245A (1.05 ± 0.06-fold; not significant, using the two-tailed unpaired Student's *t* test).

Subsequently, NBCe1 transport activity has been determined in the absence or presence of 10 µM EIPA, an inhibitor of Na^+/H^+ exchanger and either in the presence of rapamycin (Figure 5c) or in the presence of 3BDO (Figure 5d). In the presence of EIPA, pH_i recovery rate in cells transfected with NBCe1-B-S245A was significantly increased, compared to those transfected with WT-NBCe1-B in the absence (0.35 ± 0.02 pH units/min and 0.26 ± 0.01 pH units/min, respectively) or presence (0.41 ± 0.03 pH units/min and 0.15 ± 0.02 pH units/min, respectively) of rapamycin (Figure 5b,c,e). Moreover, rapamycin significantly decreased pH_i recovery rate in cells transfected with WT-NBCe1-B, compared to the untreated cells, whereas pH_i recovery rate was comparable in cells transfected with NBCe1-B-S245A in the absence or presence of rapamycin (Figure 5e). Activation of mTOR signaling had no effect on pH_i recovery rate in WT-NBCe1-B transfected cells (0.26 ± 0.02 pH units/min and 0.27 ± 0.02 pH units/min in the presence or absence of 3BDO, respectively; Figure 5b,d,e), confirming previous observations (Khakipoor et al., 2019). Similarly, pH_i recovery rate in NBCe1-B-S245A was comparable in the absence (0.44 ± 0.04 pH units/min) and presence

FIGURE 4 Effects of Ser^{245} mutations on NBCe1 activity. (a) Design of the NBCe1 (*Slc4a4*) constructs encoding NBCe1 protein with Ser^{245} substituted either with alanine or aspartate. (b) GFP intensity in cells transfected with wild-type NBCe1 (WT-NBCe1-B), NBCe1-B-S245A or NBCe1-B-S245D. a.u.: arbitrary units (not significant, using two-tailed unpaired Student's *t* test). The number of cells/cultures used in the experiments is indicated in brackets. Scale bar = 15 µm (c) Immunofluorescence for NBCe1 (red) in cells transfected (green) with either WT-NBCe1-B, NBCe1-B-S245A or NBCe1-B-S245D constructs. Scale bar = 20 µm. (d–f) Representative patterns of recovery of intracellular pH (pH_i) at pH 7.4 following a NH_4^+ pulse in HeLa cells transfected either with WT-NBCe1-B (d), NBCe1-B-S245A (e) or NBCe1-B-S245D (f) in the presence or absence of the Na^+/H^+ exchanger inhibitor EIPA (10 µM). (g) Bar plots summarizing data presented in (d–f). $^{***}p < 0.001$ for significant increase, and $^{\#}p < 0.05$ for significant decrease using one way ANOVA and Bonferroni posthoc test. The number of cells/cultures used in the experiments is indicated in brackets. ANOVA, analysis of variance; GFP, green fluorescent protein; NBCe1, Na^+/bicarbonate cotransporter 1

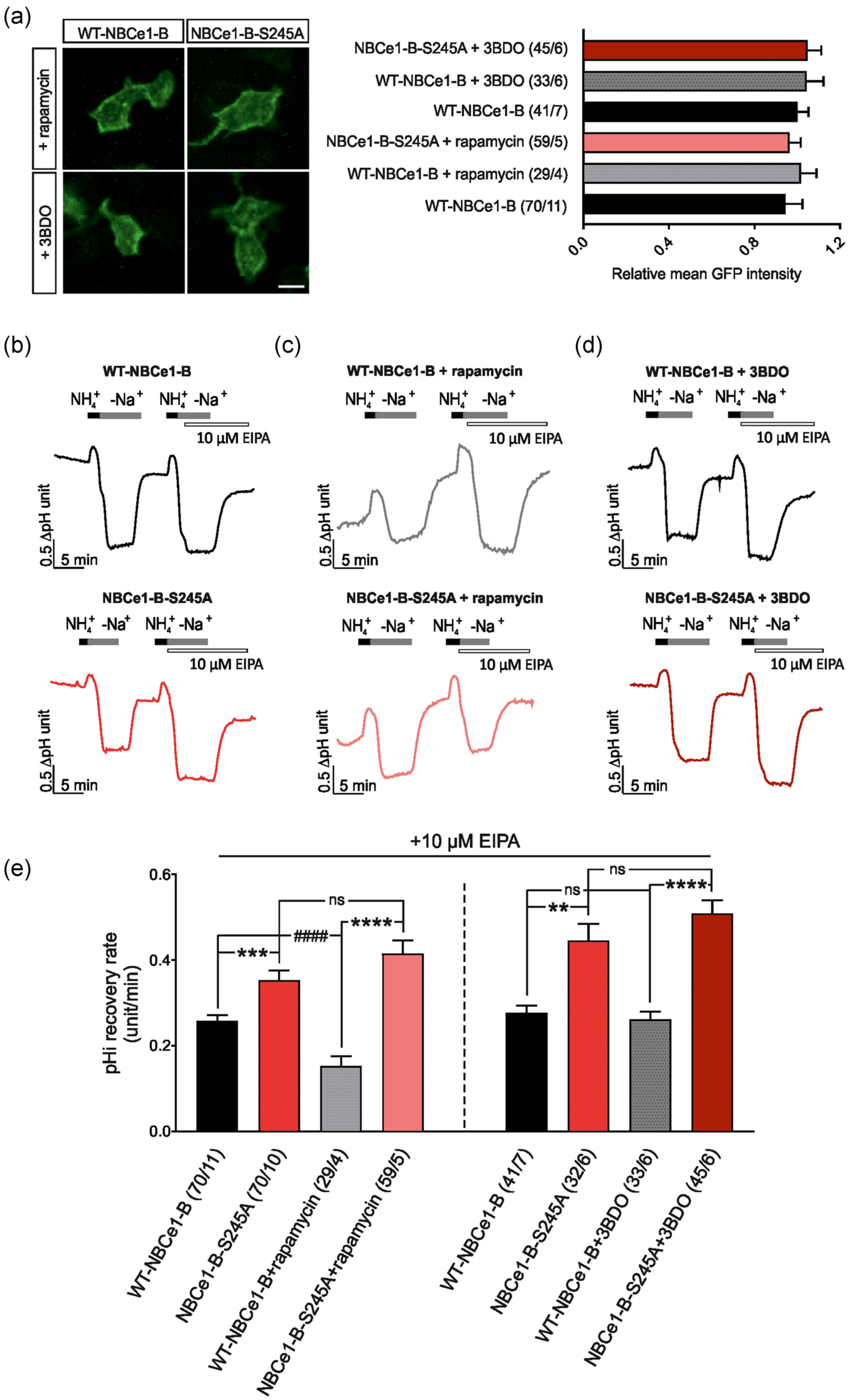

FIGURE 5 Effect of mTOR inhibition or activation on mutated NBCe1 function. (a) GFP intensity in cells transfected with wild-type NBCe1 (WT-NBCe1-B) or NBCe1-B-S245A in the presence of 1 μM rapamycin or 60 μM 3BDO (not significant, using the two-tailed unpaired Student's *t* test). Data are presented as mean ± SEM, normalized to the mean intensity of the respective WT-NBCe1-B. Scale bar = 15 μm. (b–d) Representative patterns of recovery of intracellular pH (pH_i) at pH 7.4 following a NH_4^+ pulse in the absence and presence 10 μM EIPA and with or without inhibition or activation of mTOR using rapamycin (c) or 3BDO (d) in HeLa cells transfected either with WT-NBCe1-B or with NBCe1-BS245A construct, in which Ser^{245} were substituted with alanine (c, d). (e) Bar plots showing quantification of pH recovery rate (units/min) displayed in (b–d). $^{**}p < 0.01$, $^{***}p < 0.001$, and $^{****}p < 0.0001$ for significant increase, $^{####}p < 0.0001$ for significant decrease using one way ANOVA and Bonferroni posthoc test. The number of cells/cultures used in the experiments is indicated in brackets. ANOVA, analysis of variance; EIPA, ethylisopropyl amiloride; GFP, green fluorescent protein; mTOR, mammalian target of rapamycin; NBCe1, Na^+/bicarbonate cotransporter 1

(0.50 ± 0.03 pH units/min) of 3BDO. Moreover, in the presence of 3BDO, pH_i recovery rate was significantly increased in NBCe1-B-S245A, compared to WT-NBCe1-B (Figure 5e). $^{**}p < 0.01$, $^{***}p < 0.001$, $^{****}p < 0.0001$, for significant increase, and $^{####}p < 0.0001$ for significant decrease, using one-way ANOVA and Bonferroni post hoc test.

These results suggest that mTOR pathway specifically regulates phosphorylation of Ser^{245} and thereby functional expression of NBCe1-B.

Based on these results we have asked whether acidosis-induced upregulation of NBCe1 function can be attributed to decreased phosphorylation of Ser^{245}. To that end, enriched surface proteins from control cortical astrocytes and from those exposed to extracellular acidosis in the presence or absence of rapamycin were processed for phosphoproteomic analysis. Phosphopeptide intensity for Ser^{245}, normalized to total mass spectrometric protein intensity of NBCe1, was however comparable in all experimental conditions (Figure S2a).

3.6 | Acidosis-induced increased NBCe1 functional expression is regulated by mTOR

Taken into consideration that phosphorylation of multiple serine residues on NBCe1 is specifically regulated by mTOR (Figures 4 and 5; Khakipoor et al., 2019), we have investigated the significance of inhibition of mTOR signaling on NBCe1 functional expression in the experimental setting of extracellular acidosis in mouse cortical astrocytes. Therefore, mouse cortical astrocytes were exposed to acidosis for 3 h in the presence or absence of 1 µM rapamycin, and subsequently, intracellular $[H^+]$ recordings have been performed using the same experimental design as applied for the experiments shown in Figure 3. As shown in Figure 6a,c,d, in control astrocytes (exposed to pH 7.4 for 3 h), in the presence of 1 µM rapamycin, both the rate of acidification (Figure 6a,c; 114.4 ± 8.07 nM/min) and the rate of alkalinisation (Figure 6a,d; −315.90 ± 16.56 nM/min) was significantly decreased, compared to untreated cells (186.5 ± 8.47 nM/min and −422.30 ± 20.84 nM/min, for rate of acidification and rate of alkalinisation, respectively). Similar results were also obtained in astrocytes exposed to metabolic acidosis for 3 h. The rate of acidification (Figure 6b,c; 79.48 ± 6.50 nM/min) and the rate of alkalinisation (Figure 6b,d; −257.20 ± 26.24 nM/min) was significantly decreased in the presence of rapamycin, compared to acidotic cells without rapamycin (163.4 ± 9.53 nM/min and −546.20 ± 22.69 nM/min, for rate of acidification and rate of alkalinisation, respectively). Importantly, the acidosis-induced increased rate of alkalinisation was suppressed in the presence of rapamycin and showed no significant differences to the corresponding controls (i.e., in the presence of rapamycin) $^{****}p < 0.0001$ for significant increase, $^{##}p < 0.01$, and $^{####}p < 0.0001$ for significant decrease, using one-way ANOVA and Bonferroni post hoc test.

These results strongly suggest that in mouse cortical astrocytes acidosis-induced increase in NBCe1 activity is mTOR-dependent. Interestingly, the rapamycin-induced reduced NBCe1 function cannot be attributed to changes of NBCe1 total or surface protein (Figure S2b).

4 | DISCUSSION

Local extracellular acid–base challenges during physiological and pathophysiological conditions evoke regional pH_i responses. In the brain, acidification of the extracellular space occurs during neuronal activity, but it may also accompany traumatic brain injury, local ischemia and inflammation (Gupta et al., 2004; Lipton, 1999; Yao & Haddad, 2004). Astrocytes are pivotal responders to alterations in extracellular pH, primarily by regulation of their principal acid–base transporter, the NBCe1 (Deitmer & Rose, 2010). We have previously demonstrated that following long-term extracellular metabolic alkalosis, NBCe1 transport activity is downregulated in an mTOR-dependent manner and identified phosphorylation of $Ser^{255–257}$ as being crucial for NBCe1 functional expression (Khakipoor et al., 2019).

Here we show that exposure of mouse cortical astrocytes to long-term extracellular metabolic acidosis regulates NBCe1 activity as well. The rate of alkalinisation but not the rate of acidification (Figure 3) was significantly increased compared to control astrocytes, thus conversely regulated than following exposure to metabolic alkalosis (Khakipoor et al., 2019), and was suppressed following inhibition of mTOR signaling (Figure 6). Although the experimental setting was not designed to distinguish between inward and outward directed NBCe1 these results may indicate that NBCe1 is prone to operate at the inward mode. If so, this response resembles that of pH sensitive astrocytes of the brainstem following short-term CO_2-mediated acidification (Turovski et al., 2016) but is in contrast to that of cortical astrocytes to short-term isocapnic acidosis, hypercapnic acidosis and isohydric hypocapnia (Theparambil et al., 2017), thus supporting the view of a context-dependent and cell-type dependent regulation of NBCe1 (Salameh et al., 2014). The results also show that the observed change of NBCe1 activity following extracellular metabolic acidosis is not associated with changes of total NBCe1 or surface protein abundance or with activation of astrocytes (Figures 1 and 2). Thus, these results extend our previous observations following exposure of cortical astrocytes to metabolic alkalosis (Khakipoor et al., 2019) or to extracellular acidosis by decreasing extracellular pH at constant bicarbonate concentration (Giannaki et al., 2021). Moreover, the observation that in NBCe1 deficient astrocytes of the rate of alkalinization and acidification was almost abolished, as compared to WT cells (Figure 3) highlights that NBCe1 and not Na^+/H^+ exchanger is the major regulator of intracellular pH in the presence of CO_2/HCO_3^- in astrocytes. Interestingly, although NHE1 and NHE2 mRNA is expressed in mouse cortical astrocytes (Wada et al., 2005) and NHE1 has been considered to regulate pH_i homeostasis in cortical (Kintner et al., 2004; Wang et al., 2016) and hippocampal astrocytes (Cengiz et al., 2014) under HCO_3^- free conditions, more recent studies have challenged this notion and have shown that even in the nominal absence of HCO_3^-, NBCe1 activity is present (Theparambil & Deitmer, 2015).

An important novel finding of the present work is that mTOR-mediated phosphorylation of Ser^{245} affects NBCe1 function (Figures 4d and 5). We have previously shown that $pSer^{245}$ of

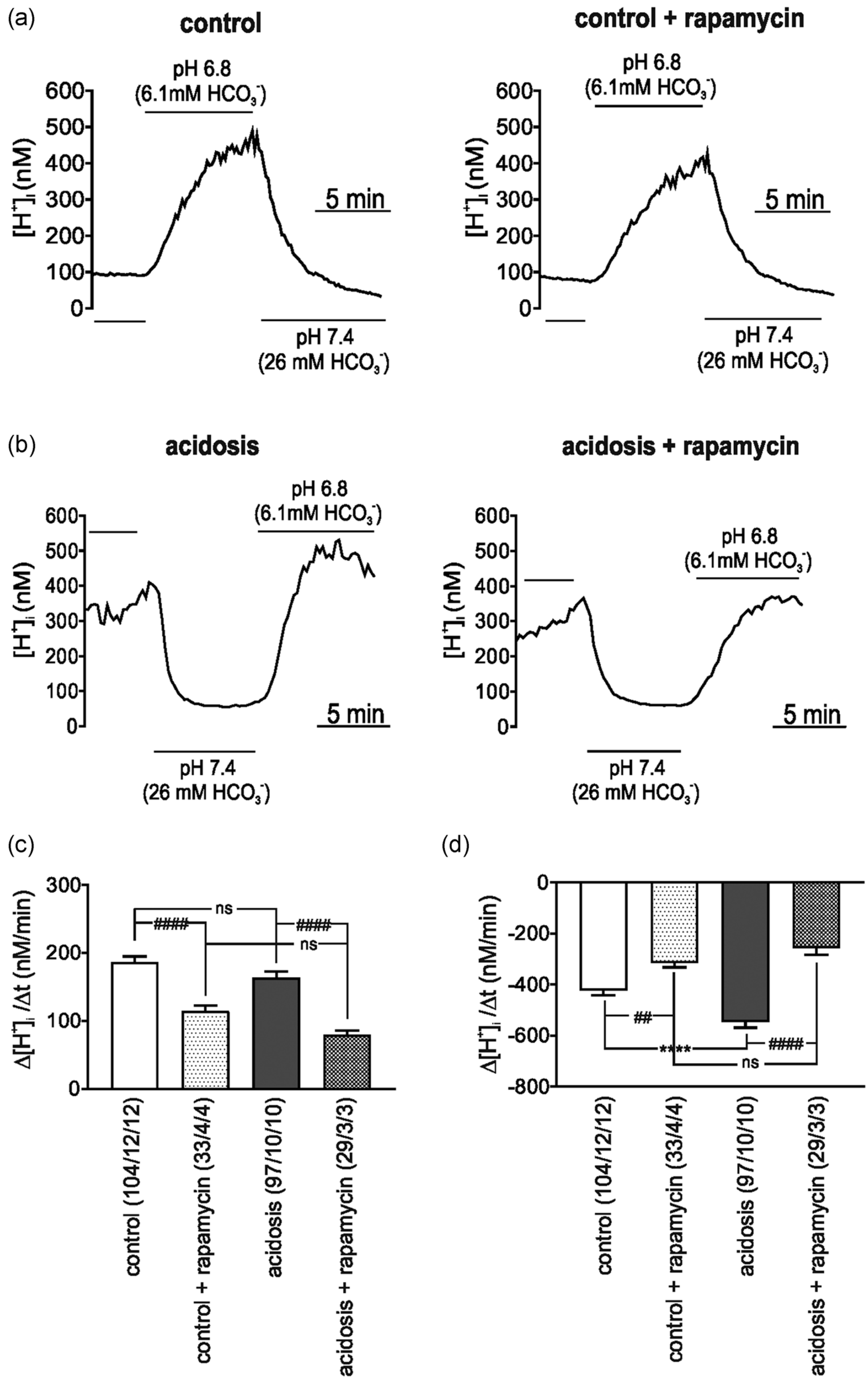

FIGURE 6 Inhibition of mTOR prevents increased NBCe1 functional expression during metabolic acidosis. Evaluation of NBCe1 transport activity. (a, b) Original recordings of intracellular $[H^+]$ ($[H^+]_i$) in cultured control cortical astrocytes (a) and in astrocytes that have been exposed to extracellular metabolic acidosis for 3 h (b) in the presence or absence of rapamycin, an inhibitor of mTOR signaling. $[H^+]_i$ was monitored during the increase of external pH and $[HCO_3^-]$ from 6.8 and 6.1 mM to 7.4 and 26.0 mM, respectively, and during the decrease of external pH and $[HCO_3^-]$ from 7.4 and 26.0 mM to 6.8 and 6.1 mM (c, d). Bar plots displaying the rate of acidification (c) and alkalinisation (d) $^{****}p < 0.0001$, for significant increase $^{\#\#}p < 0.01$, $^{\#\#\#\#}p < 0.0001$ for significant decrease, using one way ANOVA and Bonferroni posthoc test. The number of cells/cultures/animals used in the experiments is indicated in brackets. ANOVA, analysis of variance; mTOR, mammalian target of rapamycin; NBCe1, Na^+/bicarbonate cotransporter 1

NBCe1, a serine conserved in all NBCe1 variants, exerts the highest occupancy in mouse cortical astrocytes, compared to other known phosphorylation sites, such as pSer$^{255-257}$, and pSer^{232} pSer^{233} pSer^{235} (Khakipoor et al., 2019). Phosphorylation at Ser^{245} was also detected in epithelial cells (Vachel et al., 2018) and in the cerebellum (Schindler et al., 2013), strongly suggesting that NBCe1 is constitutively phosphorylated at Ser^{245}. However, whether Ser^{245} phosphorylation plays a role on NBCe1 function has not been addressed so far. Here, we have demonstrated the functional significance of Ser^{245} and its dependency on mTOR by mutational analysis (Figures 4 and 5). Loss of function experiments, that is, transfection of the cells with mutant NBCe1 mimicking the dephosphorylated state of Ser^{245} showed significant increased pH$_i$ recovery rate both in the presence or absence of rapamycin or 3BDO (Figure 5e), compared to WT NBCe1. Gain of function experiments, that is, transfection of the cells with the phosphomimetic construct showed no differences with regard to NBCe1 activity, as compared to WT (Figure 4g). Together with our previous observations on the phosphorylation state of Ser$^{255-257}$, the results demonstrate that mTOR-mediated direct phosphorylation of NBCe1 at Ser^{245} and Ser$^{255-257}$ are inversely correlated with NBCe1 functional expression. Phosphorylation of Ser$^{255-257}$ upregulates NBCe1 function (Khakipoor et al., 2019), while phosphorylation of Ser^{245} reduces NBCe1 transport activity (Figure 5). Moreover, the observation that in the presence of rapamycin NBCe1 function was downregulated in HeLa cells transfected with WT NBCe1 (Figure 5e), as well as in control and acidotic primary cortical astrocytes (Figure 6c,d), implies that the impact of reduced phosphorylation of Ser$^{255-257}$ on NBCe1 activity is likely to be functionally more relevant than that of reduced phosphorylation of Ser^{245}. It was therefore surprising that following mutation of Ser^{245} to alanine, NBCe1 functional expression was comparable in the presence or absence of rapamycin (Figure 5e). This suggests that either additional, not yet identified, phosphorylation sites may be regulated by mTOR as well or that S245A might have led to altered conformation of the transporter and indirectly affected phosphorylation of Ser$^{255-257}$. The scenario of an interdependency of phosphorylation of multiple serine residues is indeed attractive but future experiments are necessary to provide experimental evidence for this assumption.

These findings reveal how the same pathway may use context-dependent-multisite phosphorylation to fine tune the function of a given transport protein, which may have important consequences for the homeostatic regulation of brain parenchymal pH. Indeed, the early observation that glial cells control the extracellular pH in the leech central nervous system via secretion of bicarbonate (Deitmer, 1991, 1992) has been recently studied in detail in an in vivo study and identified NBCe1-mediated bicarbonate release by astrocytes as a protective mechanism against neuronal activity-associated transient extracellular acid load (Theparambil et al., 2020). In epithelial cells, since the observation that NBCe1 is a target molecule for IRBIT (inositol 1,4,5-trisphosphate [IP3] receptors binding protein released with IP3) (Shirakabe et al., 2006), several studies have elucidated the biological significance of IRBIT-regulated multiple phosphorylation sites on NBCe1. By recruitment of kinase and phosphatase pathways, differential phosphorylation of Ser^{232}, Ser^{233}, Ser^{235}, Ser^{65}, and Ser^{12} in NBCe1-B controls transporter activity and/or its regulation by intracellular Cl^- (Hong et al., 2013; Shcheynikov et al., 2015; Vachel et al., 2018). Our work has uncovered first insights on the impact of mTOR pathway as a novel regulator of NBCe1 functional properties by controlling phosphorylation of Ser^{245} and of the patch Ser^{255} Ser^{256} Ser^{257}.

mTOR-regulated NBCe1 function through phosphorylation of several residues may have important implications for fluid and electrolyte transport in epithelia- among them in the kidney. Besides the central role of mTOR pathway in the regulation of cell metabolism, growth and proliferation, many studies have uncovered additional roles of mTOR for renal cell homeostasis and tubular transport in health and disease (reviewed by Fantus et al., 2016). In mice with conditional deletion of mTORC1 in the renal proximal tubule, phosphorylation of NBCe1 at Thr^{3} (a residue in the unique N-terminal domain of NBCe1-A variant), Ser^{1060}, and Ser^{232} was reduced (Grahammer et al., 2017) but the significance of these phosphorylation sites on transporter functional properties is unknown. Since the kidney expresses both NBCe1-A and NBCe1-B (Roussa et al., 2004) and the link between proximal renal tubular acidosis and NBCe1 function is well established (Seki et al., 2013) investigation of putative mTOR-mediated alteration of NBCe1 function could reveal valuable mechanistic insights.

It is also well established that acidity and hypoxia inhibit mTORC1 activity (Balgi et al., 2011; Laplante & Sabatini, 2012). In tumors, disrupting proton dynamics and the application of mTORC1 inhibitors have been considered as promising targets for cancer therapy (Grabiner et al., 2014). As a next step, and based on the results from the mutational analysis, we have tested the hypothesis that exposure of mouse cortical astrocytes to extracellular acidosis inhibits mTORC1 pathway that in turn reduces phosphorylation of Ser^{245} of NBCe1 and leads to increased NBCe1 transport activity. Quantitative phosphoproteomics however, has not revealed any significant changes in the phosphorylation state of Ser^{245} at any experimental condition (Figure S2a). Many reasons may account for the lack of detection of phosphorylation changes. It could be that phosphorylation of Ser^{245} is not the underlying molecular mechanism for the observed acidosis-induced increase in NBCe1 activity in cortical astrocytes. In addition, methodological limitations, only partial inhibition of mTORC1 at pH 6.8 (Balgi et al., 2011), and the fact that the samples processed for phosphoproteomic analysis are derived from cells at different developmental stages with distinct functional properties should also be considered. Another explanation could be that only a subpopulation of astrocytes responds to extracellular acidosis, resembling the results obtained in vivo and in vivo following neuronal activity (Theparambil et al., 2020).

Taken together, the results of the present study identify pSer^{245} as a novel regulator of NBCe1 functional expression and that mTOR pathway has a central role in regulation of NBCe1 function. Context-dependent and mTOR-mediated multisite phosphorylation of serine residues of NBCe1 is likely to be a potent mechanism contributing to the response of astrocytes to acid/base challenges during pathophysiological conditions.

ACKNOWLEDGEMENTS

We thank Ellen Gimbel and Melanie Feuerstein for technical assistance, Gary E. Shull, Cincinnatti, USA, for providing NBCe1-KO mice and Joachim Deitmer for valuable comments on the manuscript. We acknowledge Franziska Hackbarth and Lara Wanner for technical assistance, as well as Miriam Abele for mass spectrometric support. Open access funding enabled and organized by Projekt DEAL.

CONFLICT OF INTERESTS

The authors declare that there are no conflict of interests.

ORCID

Marina Giannaki http://orcid.org/0000-0001-5761-4255
Eleni Roussa http://orcid.org/0000-0002-0495-1597

REFERENCES

Balgi, A. D., Diering, G. H., Donohue, E., Lam, K. K. Y., Fonseca, B. D., Zimmerman, C., Numata, M., & Roberge, M. (2011). Regulation of mTORC1 signaling by pH. *PLOS One*, *6*, e21549. https://doi.org/10.1371/journal.pone.0021549

Cengiz, P., Kintner, D. B., Chanana, V., Yuan, H., Akture, E., Kendigelen, P., Begum, G., Fidan, E., Uluc, K., Ferrazzano, P., & Sun, D. (2014). Sustained Na^+/H^+ exchanger activation promotes gliotransmitter release from reactive hippocampal astrocytes following oxygen-glucose deprivation. *PLOS One*, *9*, e84294. https://doi.org/10.1371/journal.pone.0084294

Ch'en, F. F.-T., Villafuerte, F. C., Swietach, P., Cobden, P. M., & Vaughan-Jones, R. D. (2008). S0859, an N-cyanosulphonamide inhibitor of sodium-bicarbonate cotransport in the heart. *British Journal of Pharmacology*, *153*, 972–982. https://doi.org/10.1038/sj.bjp.0707670

Corbet, C., & Feron, O. (2017). Tumour acidosis: From the passenger to the driver's seat. *Nature Reviews Cancer*, *17*, 577–593. https://doi.org/10.1038/nrc.2017.77

Cox, J., Neuhauser, N., Michalski, A., Scheltema, R. A., Olsen, J. V., & Mann, M. (2011). Andromeda: A peptide search engine integrated into the MaxQuant environment. *Journal of Proteome Research*, *10*(2011), 1794–1805. https://doi.org/10.1021/pr101065j

Deitmer, J. W. (1991). Electrogenic sodium-dependent bicarbonate secretion by glial cells of the leech central nervous system. *Journal of General Physiology*, *98*, 637–655.

Deitmer, J. W. (1992). Evidence for glial control of extracellular pH in the leech central nervous system. *GLIA*, *5*, 43–47. https://doi.org/10.1002/glia.440050107

Deitmer, J. W., & Rose, C. R. (1996). pH regulation and proton signaling by glial cells. *Progress in Neurobiology*, *48*, 73–103. https://doi.org/10.1016/0301-0082(95)00039-9

Deitmer, J. W., & Rose, C. R. (2010). Ion changes and signaling in perisynaptic glia. *Brain Research Reviews*, *63*, 113–129. https://doi.org/10.1016/j.brainresrev.2009.10.006

Faes, S., Duval, A. P., Planche, A., Uldry, E., Santoro, T., Pythoud, C., Stehle, J.-C., Horlbeck, J., Letovanec, I., Riggi, N., Demartines, N., & Dormond, O. (2016). Acidic tumor microenvironment abrogates the efficacy of mTORC1 inhibitors. *Molecular cancer*, *15*, 78. https://doi.org/10.1186/s12943-016-0562-y

Fantus, D., Rogers, N. M., Grahammer, F., Huber, T. B., & Thomson, A. W. (2016). Roles of mTOR complexes in the kidney: implications fir renal disease and translplantation. *Nature Reviews Nephrology*, *12*, 587–609. https://doi.org/10.1038/nrneph.2016.108

Gawenis, L. R., Bradford, E. M., Prasad, V., Lorenz, J. N., Simpson, J. E., Clarke, L. L., Woo, A. L., Grisham, C., Sanford, L. P., Doetschman, T., Miller, M. L., & Shull, G. E. (2007). Colonic anion secretory defects and metabolic acidosis in mice lacking the NBC1 Na^+/HCO_3^- cotransporter. *The Journal of Biological Chemistry*, *282*, 9042–9052. https://doi.org/10.1074/jbc.M607041200

Ge, D., Han, L., Huang, S., Peng, N., Wang, P., Jiang, Z., Zhao, J., Su, L., Zhang, S., Zhang, Y., Kung, H., Zhao, B., & Miao, J. (2014). Identification of a novel mTOR activator and discovery of a competing endogenous RNA regulating autophagy in vascular endothelial cells. *Autophagy*, *10*, 957–971. https://doi.org/10.4161/auto.28363

Giannaki, M., Schrödl-Häußel, M., Khakipoor, S., Kirsch, M., & Roussa, E. (2021). STAT3-dependent regulation of the electrogenic $Na^{+/}HCO_3^-$ cotransporter 1 (NBCe1) functional expression in cortical astrocytes. *Journal of Cellular Physiology*, *236*, 2036–2050. https://doi.org/10.1002/jcp.29990

Grabiner, B. C., Nardi, V., Birsoy, K., Possemato, R., Shen, K., Sinha, S., Jordan, A., Beck, A. H., & Sabatini, D. M. (2014). A diverse array of cancer-associated MTOR mutations are hyperactivating and can predict rapamycin sensitivity. *Cancer Discovery*, *4*, 554–563. https://doi.org/10.1158/2159-8290.CD-13-0929

Grahammer, F., Haenisch, N., Steinhardt, F., Sandner, L., Roerden, M., Arnold, F., Cordts, T., Wanner, N., Reichardt, W., Kerjaschki, D., Ruegg, M. A., Hall, M. N., Moulin, P., Busch, H., Boerries, M., Walz, G., Artunc, F., & Huber, T. B. (2014). mTORC1 maintains renal tubular homeostasis and is essential in repsonse to ischemic stress. *Proceedings of the National Academy of Sciences of the United States of America*, *111*, E2817–E2826. https://doi.org/10.1073/pnas

Grahammer, F., Nesterov, V., Ahmed, A., Steinhardt, F., Sandner, L., Arnold, F., Cordts, T., Negrea, S., Bertog, M., Ruegg, M. A., Hall, M. N., Walz, G., Korbmacher, C., Artunc, F., & Huber, T. B. (2016). mTORC2 critically regulates renal potassium handling. *The Journal of Clinical Investigation*, *126*, 1773–1782. https://doi.org/10.1172/JCI80304

Grahammer, F., Ramakrishnan, S. K., Rinschen, M. M., Larionov, A. A., Syed, M., Khatib, H., Roerden, M., Sass, J. O., Helmstaedter, M., Osenberg, D., Kühne, L., Kretz, O., Wanner, N., Jouret, F., Benzing, T., Artunc, F., Huber, T. B., & Theilig, F. (2017). mTOR regulates endocytosis and nutrient transport in proximal tubular cells. *Journal of the American Society of Nephrology*, *28*, 230–241. https://doi.org/10.1681/ASN.2015111224

Gupta, A. K., Zyygun, D. A., Johnston, A. J., Steiner, L. A., Al-Rawi, P. G., Chatfield, D., Shepherd, E., Kirkpatrick, P. J., Hutchinson, P. J., & Menon, D. K. (2004). Extracellular brain pH and outcome following severe traumatic brain injury. *Journal of Neurotrauma*, *21*, 678–684. https://doi.org/10.1089/0897715041269722

Hong, J. H., Yang, D., Shcheynikov, N., Ohana, E., Shin, D. M., & Muallem, S. (2013). Convergence of IRBIT, phosphatidylinositol (4,5) bisphosphate, and WNK/SPAK kinases in regulation of the Na^+-HCO_3^- cotransporters family. *Proceedings of the National Academy of Sciences of the United States of America*, *110*, 4105–4110. https://doi.org/10.1073/pnas.1221410110

Hsu, P. P., Kang, S. A., Rameseder, J., Zhang, Y., Ottina, K. A., Lim, D., Peterson, T. R., Choi, Y., Gray, N. S., Yaffe, M. B., Marto, J. A., & Sabatini, D. M. (2011). The mTOR-regulated phosphoproteome reveals a mechanism of mTORC1-mediated inhibition of growth factor signaling. *Science*, *332*, 1317–1322. https://doi.org/10.1126/science.1199498

Khakipoor, S., Giannaki, M., Theparambil, S. M., Zecha, J., Küster, B., Heermann, S., Deitmer, J. W., & Roussa, E. (2019). Functional expression of electrogenic sodium bicarbonate cotransporter 1 (NBCe1) in mouse cortical astrocytes is dependent on S255-257 and regulated by mTOR. *GLIA*, *67*, 2264–2278. https://doi.org/10.1002/glia.23682

Khakipoor, S., Ophoven, C., Schrödl-Häußel, M., Feuerstein, M., Heimrich, B., Deitmer, J. W., & Roussa, E. (2017). TGF-β signaling directly regulates transcription and functional expression of the electrogenic sodium bicarbonate cotransporter 1, NBCe1 (SLC4A4), via Smad4 in mouse astrocytes. *GLIA*, *65*, 1361–1375. https://doi.org/10.1002/glia.23168

Kintner, D. B., Su, G., Lenart, B., Ballard, A. J., Meyer, J. W., Ng, L. L., Shull, G. E., & Sun, D. (2004). Increased tolerance to oxygen and glucose deprivation in astrocytes from Na^+/H^+ exchanger isoform 1 null mice. *American Journal of Physiology Cell Physiology*, *287*, C12–C21. https://doi.org/10.1152/ajpcell.00560.2003

Kuo, C. J., Chung, J., Fiorentino, D. F., Flanagan, W. M., Blenis, J., & Crabtree, G. R. (1992). Rapamycin selectively inhibits interleukin-2 activation of p70 S6 kinase. *Nature*, *358*, 70–73. https://doi.org/10.1038/358070a0

Laplante, M., & Sabatini, D. M. (2012). mTOR signaling in growth control and disease. *Cell*, *149*, 274–293. https://doi.org/10.1016/j.cell.2012.03.017

Lipton, P. (1999). Ischemic cell death in brain neurons. *Physiological Reviews*, *79*, 1431–1568. https://doi.org/10.1152/physrev.1999.79.4.1431

Liu, Y., Peterson, D. A., Kimura, H., & Schubert, D. (1997). Mechanism of cellular 3-(4,5-dimethylthiazol-2-yl)-2,5-diphenyltetrazolium bromide (MTT) reduction. *Journal of Neurochemistry*, *69*, 581–593. https://doi.org/10.1046/j.1471-4159.1997.69020581.x

MacLean, B., Tomazela, D. M., Shulman, N., Chambers, M., Finney, G. L., Frewen, B., Kern, R., Tabb, D. L., Liebler, D. C., & MacCoss, M. J. (2010). Skyline: an open source document editor for creating and analyzing targeted proteomics experiments. *Bioinformatics*, *26*, 966–968. https://doi.org/10.1093/bioinformatics/btq054

Menyhárt, Á., Zölei-Szenási, D., Puskás, T., Makra, P., Orsolya, M. T., Szepes, B. É., Tóth, R., Ivánkovits-Kiss, O., Obrenovitch, T. P., Bari, F., & Farkas, E. (2017). Spreading depolarization remarkably exacerbates ischemia-induced tissue acidosis in the young and aged rat brain. *Scientific Reports*, *7*, 1154. https://doi.org/10.1038/s41598-017-01284-4

Oehlke, O., Martin, H. W., Osterberg, N., & Roussa, E. (2011). Rab11b and its effector Rip11 regulate the acidosis-induced traffic of V-ATPase in salivary ducts. *Journal of Cellular Physiology*, *226*, 638–651. https://doi.org/10.1002/jcp.22388

Oehlke, O., Schlosshardt, C., Feuerstein, M., & Roussa, E. (2012). Acidosis-induced V-ATPase trafficking in salivary ducts is initiated by cAMP/PKA/CREB pathway via regulation of Rab11b expression. *The International Journal of Biochemistry & Cell Biology*, *44*, 1254–1265. https://doi.org/10.1016/j.biocel.2012.04.018

Oehlke, O., Speer, J. M., & Roussa, E. (2013). Variants of the electrogenic sodium bicarbonate cotransporter 1 (NBCe1) in mouse hippocampal neurons are regulated by extracellular pH changes: Evidence for a Rab8a-dependent mechanism. *The International Journal of Biochemistry & Cell Biology*, *45*, 1427–1438. https://doi.org/10.1016/j.biocel.2013.04.008

Pekny, M., & Nilsson, M. (2005). Astrocyte activation and reactive gliosis. *GLIA*, *50*, 427–434. https://doi.org/10.1002/glia.20207

Rickmann, M., Orlowski, B., Heupel, K., & Roussa, E. (2007). Distinct expression and subcellular localization patterns of Na^+/HCO_3^- cotransporter (SLC4A4) variants NBCe1-A and NBCe1-B in mouse brain. *Neuroscience*, *146*, 1220–1231. https://doi.org/10.1016/j.neuroscience.2007.02.061

Roussa, E., Nastainczyk, W., & Thévenod, F. (2004). Differential expression of electrogenic NBC1 (SLC4A4) variants in rat kidney and pancreas. *Biochemical and Biophysical Research Communications*, *314*, 382–389. https://doi.org/10.1016/j.bbrc.2003.12.099

Salameh, A. I., Ruffin, V. A., & Boron, W. F. (2014). Effects of metabolic acidosis on intracellular pH responses in multiple cell types. *American Journal of Physiology Integrative Comparative Physiology*, *307*, R1413–R1427. https://doi.org/10.1152/ajpregu.00154.2014

Schindler, J., Ye, J., Jensen, O. N., & Nothwang, H. G. (2013). Monitoring the native phosphorylation state of plasma membrane proteins from a single mouse cerebellum. *Journal of Neuroscience Methods*, *213*, 153–164. https://doi.org/10.1016/j.jneumeth.2012.10.003

Seki, G., Horita, S., Suzuki, M., Yamazaki, O., Usui, T., Nakamura, M., & Yamada, H. (2013). Molecular mechanisms of renal and extrarenal manifestations caused by inactivation of the electrogenic Na^+-HCO_3^- cotransporter NBCe1. *Frontiers in Physiology*, *4*, 270. https://doi.org/10.3389/fphys.2013.00270

Sharma, V., Eckels, J., Schilling, B., Ludwig, C., Jaffe, J. D., MacCoss, M. J., & MacLean, B. (2018). Panorama public: A public repository for quantitative data sets processed in skyline. *Molecular Cell Proteomics*, *17*, 1239–1244. https://doi.org/10.1074/mcp.RA117.000543

Shcheynikov, N., Son, A., Hong, J. H., Yamazaki, O., Ohana, E., Kurtz, I., Shin, D. M., & Muallem, S. (2015). Intracellular Cl^- as a signaling ion that potently regulates Na^+/HCO_3^- transporters. *Proceedings of the National Academy of Sciences of the United States of America*, *112*, E329–E337. https://doi.org/10.1073/pnas.1415673112

Shevchenko, A., Tomas, H., Havlis, J., Olsen, J. V., & Mann, M. (2006). In-gel digestion for mass spectrometric characterization of proteins and proteomes. *Nature Protocols*, *1*, 2856–2860. https://doi.org/10.1038/nprot.2006.468

Shirakabe, K., Priori, G., Yamada, H., Ando, H., Horita, S., Fujita, T., Fujimoto, I., Mizutani, A., Seki, G., & Mikoshiba, K. (2006). IRBIT, an inositol 1,4,5-trisphosphate receptor-binding protein, specifically binds to and activates pancreas-type Na^+/HCO_3^- cotransporter 1 (pNBC1). *Proceedings of the National Academy of Sciences of the United States of America*, *103*, 9542–9547. https://doi.org/10.1073/pnas.0602250103

Theparambil, S. M., & Deitmer, J. W. (2015). High effective cytosolic H^+ buffering in mouse cortical astrocytes attributable to fast bicarbonate transport. *GLIA*, *63*, 1581–1594. https://doi.org/10.1002/glia.22829

Theparambil, S. M., Hosford, P. S., Ruminot, I., Kopach, O., Reynolds, J. R., Sandoval, P. Y., Rusakov, D. A., Barros, L. F., & Gourine, A. V. (2020). Astrocytes regulate brain extracellular pH via a neuronal activity-dependent bicarbonate shuttle. *Nature Communications*, *11*, 5073. https://doi.org/10.1038/s41467-020-18756-3

Theparambil, S. M., Naoshin, Z., Defren, S., Schmaelzle, J., Weber, T., Schneider, H. P., & Deitmer, J. W. (2017). Bicarbonate sensing in mouse cortical astrocytes during extracellular acid/base disturbances. *The Journal of Physiology*, *595*, 2569–2585. https://doi.org/10.1113/JP273394

Theparambil, S. M., Naoshin, Z., Thyssen, A., & Deitmer, J. W. (2015). Reversed electrogenic sodium bicarbonate cotransporter 1 is the major acid loader during recovery from cytosolic alkalosis in mouse cortical astrocytes. *The Journal of Physiology*, *593*, 3533–3547. https://doi.org/10.1113/JP270086

Theparambil, S. M., Ruminot, I., Schneider, H. P., Shull, G. E., & Deitmer, J. W. (2014). The electrogenic sodium bicarbonate cotransporter NBCe1 is a high-affinity bicarbonate carrier in cortical astrocytes. *The Journal of Neuroscience*, *34*, 1148–1157. https://doi.org/10.1523/JNEUROSCI.2377-13.2014

Turovski, E., Theparambil, S. M., Kasymov, V., Deitmer, J. W., Gutierrez der Arroyo, A., Ackland, G. L., Corneveaux, J. J., Allen, A. N., Huentelman, M. J., Kasparov, S., Marina, N., & Gourine, A. V. (2016). Mechanism of CO_2/H^+ sensitivity of astrocytes. *The Journal of Neuroscience*, *36*, 10750–10758. https://doi.org/10.1523/JNEUROSCI.1281-16.2016

Tyanova, S., Temu, T., & Cox, J. (2016). The MaxQuant computational platform for mass spectrometry-based shotgun proteomics. *Nature Protocols*, *11*, 2301–2319. https://doi.org/10.1038/nprot.2016.136

Vachel, L., Shcheynikov, N., Yamazaki, O., Fremder, M., Ohana, E., Son, A., Shin, D. M., Yamazaki-Nakazawa, A., Yang, C.-R., Knepper,, M. A., Muallem, & S. (2018). Modulation of Cl^- signaling and ion transport by recruitment of kinases and phosphatases mediated by the regulatory protein IRBIT. *Science Signaling*, *11*, eaat5018. https://doi.org/10.1126/scisignal.aat5018

Wada, M., Miyakawa, S., Shimada, A., Okada, N., Yamamoto, A., & Fujita, T. (2005). Functional linkage of H^+/peptide transporter PEPT2 and Na^+/H^+ exchanger in primary cultures from mouse cerebral cortex. *Brain Research*, *1044*, 33–41. https://doi.org/10.1016/j.brainres.2005.02.064

Wang, P., Li, L., Zhang, Z. Z., Kann, Q., Gao, F., & Chen, S. (2016). Time-dependent activity of Na^+/H^+ exchanger isoform 1 and homeostasis of intracellular pH in astrocytes exposed to $CoCl_2$ treatment. *Molecular Medicine Reports*, *13*, 4443–4450. https://doi.org/10.3892/mmr.2016.5067

Yang, D., Li, Q., So, I., Huang, C. L., Ando, H., Mizutani, A., Seki, G., Mikoshiba, K., Thomas, P. J., & Muallem, S. (2011). IRBIT governs epithelial secretion in mice by antagonizing the WNK/SPAK kinase pathway. *The Journal of Clinical Investigation*, *121*, 956–965. https://doi.org/10.1172/JCI43475

Yang, D., Shcheynikov, N., Zeng, W., Ohana, E., So, I., Ando, H., Mizutani, A., Mikoshiba, K., & Muallem, S. (2009). IRBIT coordinates epithelial fluid and HCO3- secretion by stimulating the transporters pNBC1 and CFTR in the murine pancreatic duct. *The Journal of Clinical Investigation*, *119*, 193–202. https://doi.org/10.1172/JCI36983

Yao, H., & Haddad, G. G. (2004). Calcium and pH homeostasis in neurons during hypoxia and ischemia. *Cell Calcium*, *36*, 247–255. https://doi.org/10.1016/j.ceca.2004.02.013

SUPPORTING INFORMATION

Additional supporting information may be found in the online version of the article at the publisher's website.

How to cite this article: Giannaki, M., Ludwig, C., Heermann, S., & Roussa, E. (2022). Regulation of electrogenic Na^+/HCO_3^- cotransporter 1 (NBCe1) function and its dependence on m-TOR mediated phosphorylation of Ser^{245}. *Journal of Cellular Physiology*, 237, 1372–1388. https://doi.org/10.1002/jcp.30601